

STATUS OF MQXFB QUADRUPOLE MAGNETS FOR HL-LHC

A. Milanese¹, G. Ambrosio², G. Apollinari², J. Axensalva¹, M. Baldini², A. Ballarino¹, C. Barth¹, R. Carcagno², M. Crouvizier¹, A. Devred¹, D. Duarte Ramos¹, S. Feher², P. Ferracin³, J. Ferradas Troitino¹, L. Fiscarelli¹, M. Guinchard¹, S. Izquierdo Bermudez¹, N. Lusa¹, F. Mangiarotti¹, A. Moros¹, C. Petrone¹, H. Prin¹, R. Principe¹, E. Ravaioli¹, P. Rogacki¹, P. Quassolo¹, S. Russenschuck¹, S. Sgobba¹, T. Strauss³, E. Todesco¹, A. Vouris², G. Willering¹
¹CERN, Genève, Switzerland ²FNAL, Batavia, IL 60510, USA ³LBNL, Berkeley, CA 94720, USA

Abstract

The MQXFB magnets are superconducting quadrupoles with a nominal coil peak field of 11.3 T. With a magnetic length of 7.2 m, they stand as the longest Nb₃Sn accelerator magnets designed and manufactured up to now. Together with the companion MQXFA 4.2 m long units, built by the US HL-LHC Accelerator Upgrade Project (AUP), they are at the heart of HL-LHC, to replace the inner triplet quadrupoles in the ATLAS and CMS interaction regions of the LHC. We provide here a status on MQXFB magnets, starting with powering tests. The last two quadrupoles satisfy the project requirements, with one unit also passing a comprehensive endurance test. We then report results of electrical tests and magnetic measurements, as well as changes being explored for the coil fabrication.

INTRODUCTION AND REQUIREMENTS

The High Luminosity Large Hadron Collider (HL-LHC) is a project in construction at CERN [1]. Its main objective is to extend the physics potential of the LHC by a tenfold increase of the luminosity for the ATLAS and CMS experiments. As part of this upgrade, the two interaction regions will undergo a complete reconfiguration, with the low- β triplets Nb-Ti quadrupoles MQXA and MQXB [2] replaced with larger aperture magnets, MQXFA and MQXFB [3-5], using Nb₃Sn technology. Table 1 lists the main parameters of these quadrupoles; their design, including the peculiarity of a bladder-and-key structure, is described in detail in the references.

MQXFA/B share the same cross-section and conductor [6, 7], and they are based on a common US / CERN development, through several 1.2 m long MQXFS models [8].

The HL-LHC acceptance requirements for individual MQXFB magnets – not considering special type tests – are multiple, and many are based on adhering to a Manufacturing and Inspection Plan, defined within a QA/QC framework. We focus here on a subset of requirements:

- current: to reach (at 20 A/s) and hold nominal current (I_{nom} , 16.23 kA) + 300 A at 1.9 K, with no specifications on the virgin training and up to 3 quenches to reach I_{nom} after a thermal cycle
- voltage withstand levels: in particular, high voltage (HV) between coil(s) / ground / quench heaters (QHs), at room temperature, at 1.9 K and also at 100 K, in 1.3 bar gaseous helium [9]
- magnetic field: integrated gradient and multipoles, as in [3]

These quadrupoles are also tested at 4.5 K, up again to $I_{\text{nom}} + 300$ A, to probe the margin. In the machine, at nominal condition and in the most exposed regions, the coil temperature is expected to rise not above 2.22 K [10].

Up to date, four MQXFB magnets have been manufactured and tested: MQXFBP1, MQXFBP2, MQXFBP3 and MQXFB02. The first three are prototypes and their results have already been reported extensively in [5] and [11-13]. The last one – that is, B02 – was tested in Nov. 2022 - Mar. 2023; its results, including an endurance test, are covered in the next section in more detail. All magnets so far were assembled in a standalone test cold mass / cryostat configuration, different with respect to the final Q2 layout: this allowed a faster assembly and testing. All these units have been fully manufactured at CERN, with components procured in the industry. This strategy will be kept for the rest of the series production.

In the following, we report the power test results, commenting in parallel on the evolution of the manufacturing. Then we provide results for HV electrical tests and magnetic measurements, followed by comments on coil fabrication, before giving a final outlook.

Among other things, protection (the stored energy density in the coil is 50% higher than for LHC main dipoles), mechanical aspects (strain measurements, finite element simulations), metrology and alignment, electrical resistance of splices, and VI measurements [14] (to detect hints of superconductor limitations when approaching the critical surface) are beyond the scope of this paper.

Table 1: Nominal Parameters for LHC and HL-LHC Interaction Region Quadrupoles, for 7 TeV Beam Energy

Magnet	LHC		HL-LHC	
	MQXA	MQXB	MQXFA	MQXFB
Technology	Nb-Ti		Nb ₃ Sn	
Aperture dia. [mm]	70		150	
Gradient [T/m]	215		132	
Coil peak field [T]	8.5	8.2	11.3	
Magn. length [m]	6.4	5.5	4.2	7.2
Current [kA]	7.15	11.95	16.23	
Temperature* [K]	1.9		1.9	
Loadline fraction [/]	0.79	0.82	0.77	
Stored energy [MJ]	2.30	1.36	4.91	8.37
Protection	QHs		QHs, CLIQ	
Built by	KEK	FNAL	US-AUP	CERN
Units in IP1 + IP5	8	8	16	8

* temperature increase due to collision debris not considered

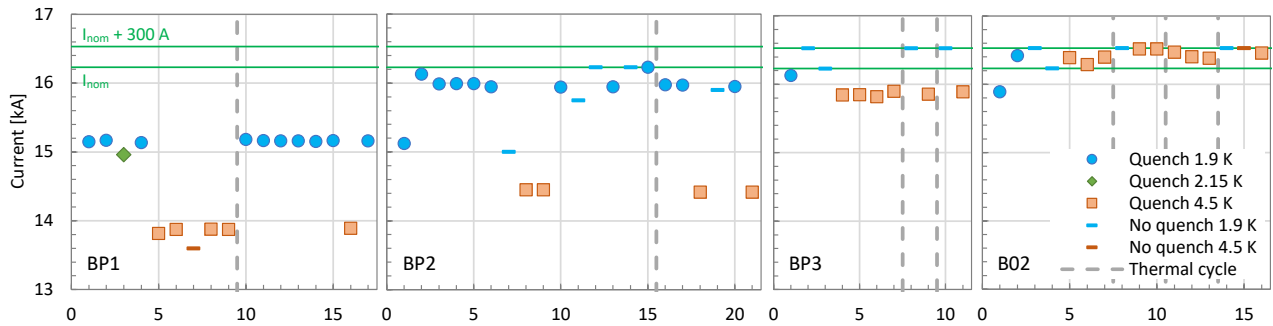


Figure 1: Natural quench history of the first four MQXFB magnets at 20 A/s.

MANUFACTURING HISTORY AND QUENCH PERFORMANCE

MQXFBP1 reached 15.17 kA (93.5% of I_{nom}) at 1.9 K with no training, and it was limited at this current in the inner layer pole turn straight section (IPTs) of a specific coil. Tests at 4.5 K showed a limitation in the same location at the same short sample current fraction. The performance was unchanged after a thermal cycle. Destructive examinations of the limiting coil showed collapsed filaments at various winding poles segments transitions, in the longitudinal center, particularly severe around the quench origin [15].

MQXFBP2 was manufactured very similarly to BP1, besides a b_6 correction on the coils and a shorter 3rd plateau in the heat treatment (to improve the RRR). The behavior of this magnet was better, but qualitatively similar to the previous one: limitation in one coil in the IPTs at 15.95 kA (98.3% of I_{nom}) – this time with a training quench – limitation at 4.5 K at the same short sample fraction and no changes after a thermal cycle. A novel method, with a current trim, allowed to probe the behavior of the other coils beyond 15.95 kA: two of them had similar limits, albeit at higher current, again in the IPTs [12].

After the results of BP1 and BP2, the production was stopped, to allow a full analysis of the root cause of the observed limitations, and to address it. A staged plan to cover a) cold mass assembly, b) magnet assembly and loading, c) coil fabrication was put in place [5].

MQXFBP3 implemented part a) above. Originally MQXFB01, it was renamed after disassembling the cold mass (already assembled at the time of the production stop), to mechanically decouple the stainless-steel liquid helium vessel from the magnet itself and its aluminum cylinders. As it was initially foreseen as the first series magnet, the coils did not include any internal voltage taps; quench localization, both longitudinally and transversally, was still possible thanks to the development of a quench antenna. BP3 reached the target current of $I_{nom} + 300$ A at 1.9 K with one training quench, and it attained again that current without quench after two thermal cycles. At 4.5 K, the magnet showed a performance limitation in the IPTs of one coil, similar to the two previous magnets, closer to I_{nom} (0.38 kA below).

MQXFB02 included parts a) and b) above, with in particular a revised procedure to apply the preload at room

temperature, to eliminate overshoots in the coil stresses observed in previous magnets [16]. B02 reached I_{nom} at 1.9 K with one quench, and the target $I_{nom} + 300$ A with a second one. Like BP3, this magnet exhibited no retraining after thermal cycles. At 4.5 K, B02 attained I_{nom} without quench, but showed a performance limitation at 16.4 kA in the IPTs of one coil, towards the mechanical center of the magnet (as for the previous ones). Like BP3, VI measurements did not show an early transition. To further probe the robustness of this magnet, we then carried out an extensive endurance test, including 36 quenches at or above I_{nom} , 508 current cycles to above I_{nom} , and a total of four cooldowns from room temperature to 1.9 K. The performance of the magnet was unchanged after such endurance tests.

Fig. 1 gives the overall quench performance at 20 A/s for these four magnets. The phenomenology is similar: short training (up to two quenches) till the target or limit current is reached, no retraining after thermal cycle(s), no degradation after thermal or powering cycles (including multiple ones, as the endurance test demonstrated), limitation in equivalent locations (IPTs) and no quenches originating in the heads. The current limit is plotted in Fig. 2 as a function of temperature, overlaid with scaled critical curves and a vertical line at the maximum expected coil temperature in the machine. Extrapolating from the results of the first two prototypes, the limiting current at 1.9 K in BP3 / B02 shall reach / exceed I_{ult} . These results show so far a consistent improvement of quench behavior, in terms of maximum attainable current. In this respect, BP3 and B02 were the first MQXFB magnets to satisfy HL-LHC requirements.

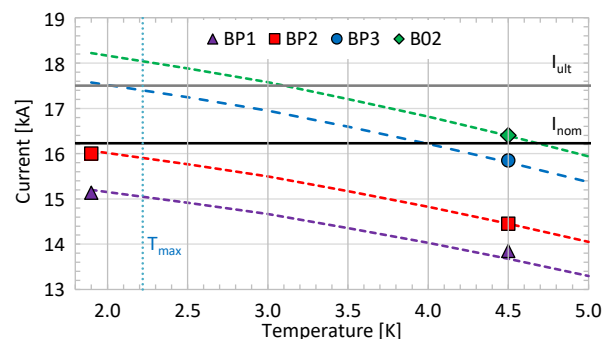


Figure 2: Limiting current vs. temperature for the first four MQXFB magnets at 20 A/s; the dashed curves are the short sample current, scaled to match the various limits.

ELECTRICAL TESTS

All HV electrical tests in the four magnets successfully passed. Still, to increase the QH-to-coil dielectric robustness, we studied a “mini-swap” QH layout, with a fresh 50- μm fiberglass sheet added before impregnation in between the QH and the coil. At the same time, the QH itself is covered by a polyimide coverlay. The thickness of the fiberglass layers on the outer layer of the coil is then adjusted to have the same pile-up. This configuration has been tested in a short model, to validate both manufacturing details and the protection delay. It has also been introduced in a MQXFB copper coil and it is now part of the baseline design.

MAGNETIC MEASUREMENTS RESULTS

We performed magnetic measurements both at room temperature and at 1.9 K, with rotating coils and a stretched wire system. We focus here on the transfer function (TF, as integrated gradient over current) and integrated multipoles; in many cases, more data is available, such as a longitudinal characterization (position of the magnetic axis, tilt and multipoles), field stability during long plateaus, effects linked to cycling, and additional measurements at room temperature during disassembly or reconfiguration of the prototypes.

Table 2 reports the TF for the first four MQXFB magnets. Data at other currents, not reported here, confirm the good reproducibility of the integrated gradient across the four magnets, of the order of $20 \cdot 10^{-4}$, as well as agreement with the saturation expected from simulations.

In Fig. 3 we plot the measured multipoles, at room temperature and at 1.9 K. These results also point to a reproducible behavior, with values at high current within a few 10^{-4} . In particular, the tuning of the coil geometry implemented since BP2 was effective in improving the b_6 . Magnetic shimming, to correct low order terms, was already proven on short magnets; this technique was applied also to MQXFB, in BP2 and B02, to correct b_3 and a_3 .

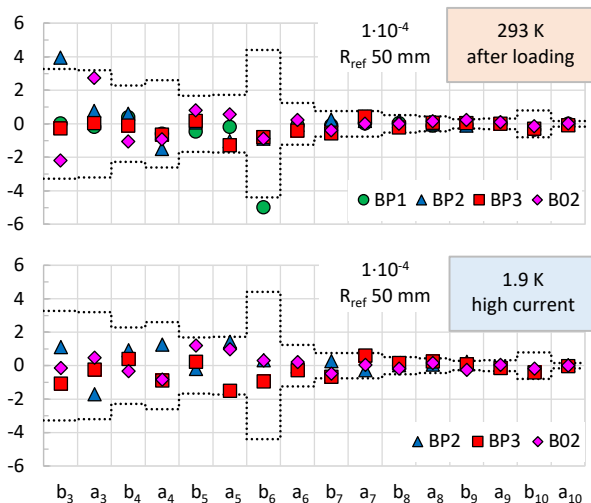


Figure 3: Integrated multipoles for the first four MQXFB; 15 kA for BP2, 16.23 kA for BP3 and B02; the dotted lines refer to the target field quality for nominal HL-LHC optics.

Table 2: Measured Magnetic Transfer Functions, at Room Temperature After Loading and at 1.9 K

TF	293 K	1.9 K 960 A	1.9 K 16230 A
BP1 [T/kA]	63.394	n. a.	59.427*
BP2 [T/kA]	63.359	n. a.	58.862*
BP3 [T/kA]	63.328	64.282	58.620
B02 [T/kA]	63.407	64.308	58.649
avg. [T/kA]	63.372	64.295	58.635

* 13.6 / 15.75 kA for BP1 / BP2, not included in the average

CHANGES IN COIL FABRICATION

We have indications that the performance limitations in the first prototypes – in terms of maximum achievable currents – are linked to damages in the Nb₃Sn conductor taking place during coil manufacturing. Such damages can in fact be observed also in virgin coils [15]. As discussed in [5], the production restarted gradually in Mar. 2022, with transition coils including additional measurements and diagnostics (like logging of mechanical and geometrical parameters), as well as modifications to the procedures.

Recent measurements showed that MQXFB coils are in a constrained state after heat treatment. This induces displacements and stress concentrations in a reacted though not yet impregnated configuration, particularly pronounced at the pole-to-pole transitions, matching the recurrent locations of quench origin and conductor damage. Such an effect seems related to the thermomechanical behavior during the heat treatment, involving phenomena like matrix annealing and phase change during formation of Nb₃Sn. This interplay with the reaction fixture, through friction, is quite complex and what we observe might be a length effect, not applicable to MQXFA and MQXFS.

Recent changes in coil manufacturing, notably in the curing after winding, before reaction, showed a promising impact for reducing the mentioned stored mechanical energy after heat treatment. This also translated, in finished impregnated coils, in a more uniform azimuthal size along the length. This work is still ongoing and a validation with tests at cryogenic temperature is in the pipeline.

CONCLUSIONS

The last two MQXFB magnets meet the HL-LHC requirements, in particular reaching 7 TeV equivalent current with a 300 A margin, and no retraining after thermal cycles. In addition, the recent endurance test confirms the robustness of the performance. As part of the three-legged strategy (cold mass, magnet, coil) – addressing the performance limitations of the first prototypes – we are now entering the last phase, focused on coil. Results on this front are expected by the end of the year, with the test of MQXFB03, which incorporates four coils of a different generation.

ACKNOWLEDGEMENTS

We gratefully acknowledge the work of the technical teams at CERN, for both manufacturing and testing. We are also thankful for the regular, open and fruitful exchanges with AUP colleagues in the US.

REFERENCES

- [1] I. Béjar *et al.* (Eds.), “High-Luminosity Large Hadron Collider (HL-LHC): Technical Design Report,” CERN Yellow Reports CERN-2020-010, Oct. 2020.
- [2] O. Brüning *et al.* (Eds.), “LHC Design Report, Vol. I, The LHC Main Ring,” CERN-2004-003, Jun. 2004.
- [3] P. Ferracin *et al.*, “Development of MQXF: the Nb₃Sn low-beta quadrupole for the HiLumi LHC,” *IEEE Trans. Appl. Supercond.*, v. 26, n. 4, Jun. 2016.
- [4] G. Ambrosio *et al.*, “Challenges and Lessons Learned from Fabrication, Testing and Analysis of Eight MQXFA Low Beta Quadrupole magnets for HL-LHC,” *IEEE Trans. Appl. Supercond.*, v. 33, n. 5, Aug. 2023.
- [5] S. Izquierdo Bermudez *et al.*, “Status of the MQXFB Nb₃Sn Quadrupoles for the HL-LHC,” *IEEE Trans. Appl. Supercond.*, v. 33, n. 5, Aug. 2023.
- [6] L. D. Cooley *et al.*, “Conductor specification and validation for High-Luminosity LHC quadrupole magnets,” *IEEE Trans. Appl. Supercond.*, v. 27, n. 4, Jun. 2017.
- [7] J. Fleiter *et al.*, “Optimization of Nb₃Sn Rutherford cables geometry for the High-Luminosity LHC,” *IEEE Trans. Appl. Supercond.*, v. 27, n. 4, Jun. 2017.
- [8] G. Vallone *et al.*, “Summary of the Mechanical Performances of the 1.5 m Long Models of the Nb₃Sn Low- β Quadrupole MQXF,” *IEEE Trans. Appl. Supercond.*, v. 29, n. 5, Aug. 2019.
- [9] M. Bednarek *et al.*, “Electrical Design Criteria for the HL-LHC inner triplet magnets,” CERN EDMS 1963398 v. 6.0, Nov 2021.
- [10] P. Borges de Sousa *et al.*, “Numerical Assessment of the Inhomogeneous Temperature Field and the Quality of Heat Extraction of Nb₃Sn Impregnated Magnets for the High Luminosity Upgrade of the LHC,” *IEEE Trans. Appl. Supercond.*, v. 33, n. 5, Aug. 2023.
- [11] S. Izquierdo Bermudez *et al.*, “Progress in the Development of the Nb₃Sn MQXFB Quadrupole for the HiLumi Upgrade of the LHC,” *IEEE Trans. Appl. Supercond.*, v. 31, n. 5, Feb. 2021.
- [12] F. J. Mangiarotti *et al.*, “Power test of the first two HL-LHC insertion quadrupole magnets built at CERN,” *IEEE Trans. Appl. Supercond.*, v. 32, n. 6, Sept. 2022.
- [13] E. Todesco *et al.*, “Status and Challenges of the Interaction Region Magnets for HL-LHC,” *IEEE Trans. Appl. Supercond.*, v. 33, n. 5, Aug. 2023.
- [14] R. Keijzer *et al.*, “Modelling V-I Measurements of Nb₃Sn Accelerator Magnets with Conductor Degradation,” *IEEE Trans. Appl. Supercond.*, v. 32, n. 6, Sept. 2022.
- [15] A. Moros *et al.*, “A Metallurgical Inspection Method to Assess the Damage in Performance-Limiting Nb₃Sn Accelerator Magnet Coils,” *IEEE Trans. Appl. Supercond.*, v. 33, n. 5, Aug. 2023.
- [16] J. Ferradas Troitino *et al.*, “Optimizing the use of pressurized bladders for the assembly of HL-LHC MQXFB magnets,” *Superconductor Science and Technology*, vol. 36, no. 6. IOP Publishing, p. 065002, Apr. 19, 2023. doi:10.1088/1361-6668/acc366